Supplementary Information for

Direction-resolved radiation from polarization-controlled surface plasmon modes on silver nanowire antennas

Zhili Jia,[a] Hong Wei,*[a] Deng Pan[b] and Hongxing Xu[b,c]

[a]Beijing National Laboratory for Condensed Matter Physics, Institute of Physics, Chinese Academy of Sciences, Beijing 100190, China

[b]School of Physics and Technology, Wuhan University, Wuhan 430072, China

[c]Institute for Advanced Studies, Wuhan University, Wuhan 430072, China

*E-mail: weihong@iphy.ac.cn

1. The calculated charge distributions of longitudinal and transverse modes on glass-supported Ag NW

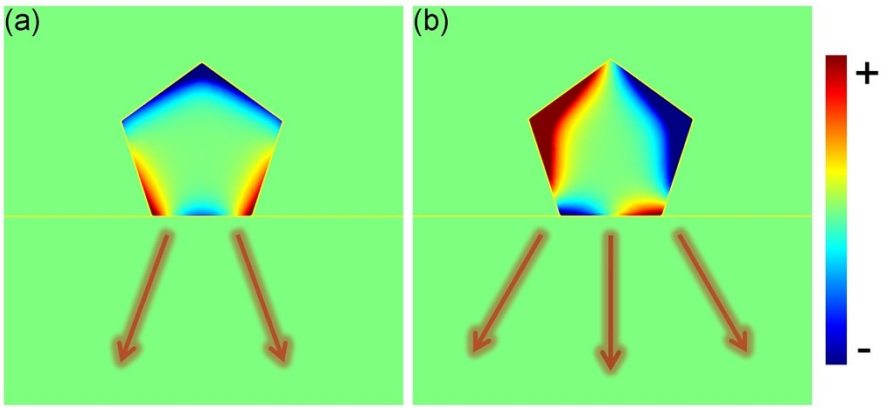

Figure S1. The calculated charge distributions of longitudinal (a) and transverse (b) modes on glass-supported Ag NW. The arrows denote the directions of radiation. The wavelength is 532 nm. The NW radius is 170 nm.

2. The emission polarization characteristics of leakage radiation from longitudinal and transverse modes

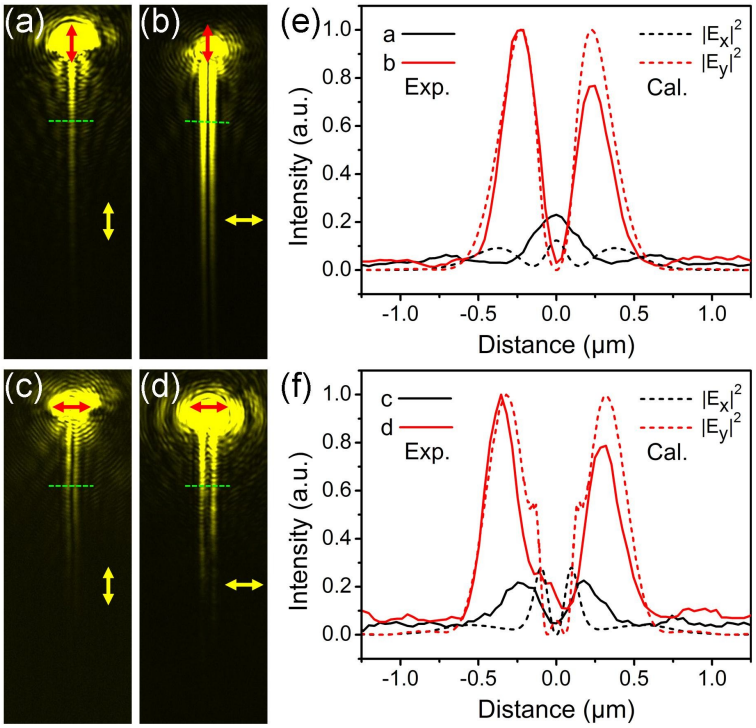

Figure S2. The intensity distributions of leakage radiation of different polarizations for longitudinal and transverse modes. (a-d) The leakage radiation images of longitudinal (a, b) and transverse (c, d) modes (the same as the images in Figure 3). (e, f) Solid curves: the intensity distributions along the green dashed lines in the corresponding leakage radiation images. Dashed curves: the simulated $|E_x|^2$ and $|E_y|^2$ distributions along the line 50 nm below the glass surface. The wavelength is 532 nm. The NW radius in simulation is 170 nm.

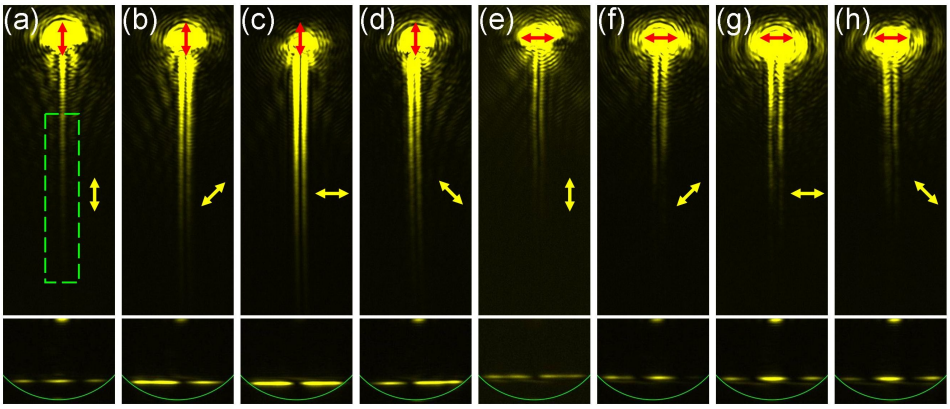

Figure S3. The emission polarization characteristics of leakage radiation from

longitudinal (a-d) and transverse (e-h) modes. Top and bottom panels are the leakage radiation images and corresponding Fourier images, respectively. The red arrows indicate the polarizations of 532 nm wavelength laser light. The yellow arrows indicate the emission polarizations. Fourier images are obtained from the area marked by the green dashed rectangle in (a). The green circles in the Fourier images represent the maximum radiation angle that can be collected by the experimental system. The exposure time of Fourier image in (e) is 300 ms, and for all the other images is 200 ms. The intensity range for the color scale of the images in (e) is 0-180, and for others is 0-360.

3. The radiation from transverse mode on a Ag NW with 30 nm Al_2O_3 film

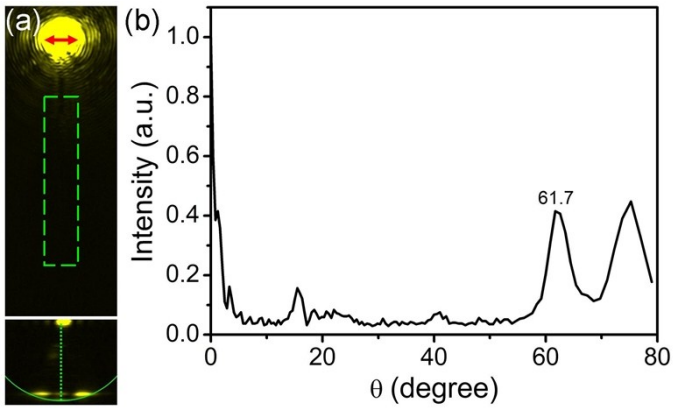

Figure S4. The radiation from transverse mode on a Ag NW coated by an Al_2O_3 layer of 30 nm thickness. (a) Leakage radiation image (top) and Fourier image (bottom). The red arrow indicates the polarization of 532 nm wavelength laser light. The Fourier image is obtained from the area marked by the green dashed rectangle in the leakage radiation image. The exposure time of leakage radiation image and Fourier image is 100 ms and 600 ms, respectively. (b) Intensity distribution versus θ along φ = 0 as marked by the green dashed line in the Fourier image.

4. The electric field distributions of two modes for different Al_2O_3 thicknesses

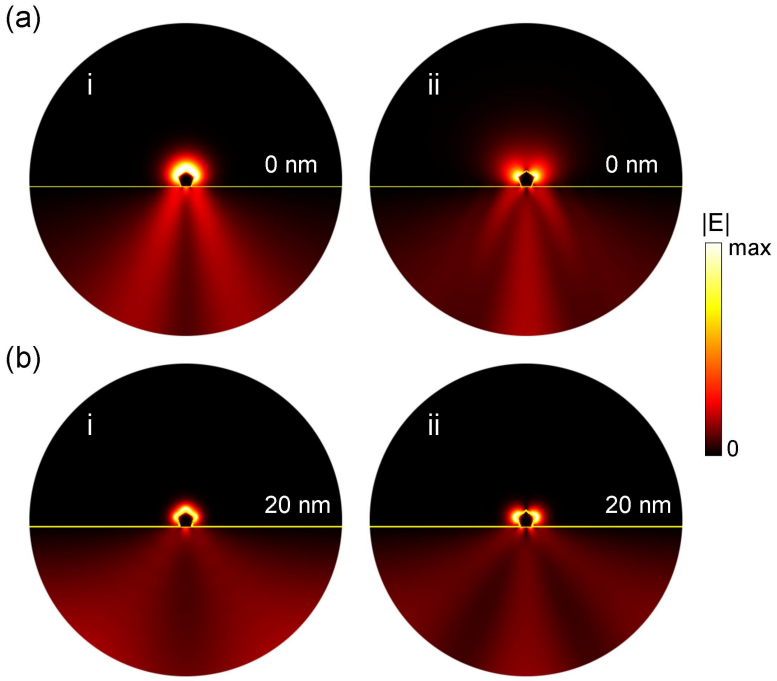

Figure S5. The electric field distributions of longitudinal mode (ai, bi) and transverse mode (aii, bii) of SPs on glass-supported Ag NWs for Al_2O_3 thickness of 0 nm (a) and 20 nm (b). The excitation wavelength is 532 nm. The NW radius is 170 nm.

5. The leakage radiation dependence on the excitation wavelength

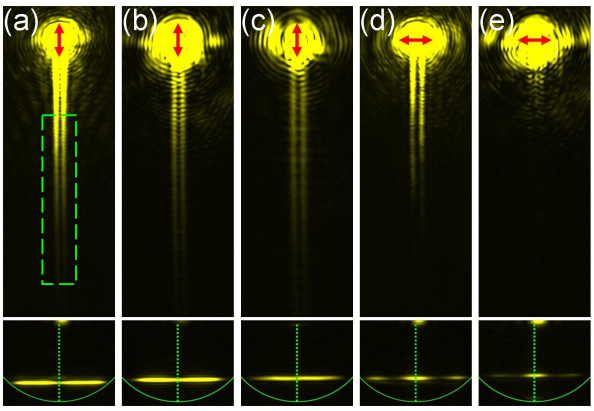

Figure S6. The leakage radiation images (top) and corresponding Fourier images (bottom) for longitudinal (a-c) and transverse (d, e) modes under different laser wavelengths [532 nm for (a) and (d), 633 nm for (b) and (e), and 785 nm for (c)]. The red arrows indicate the polarizations of the incident light. Fourier images are obtained from the area marked by the green dashed rectangle in (a). The exposure time of the

Fourier image in (e) is 600 ms, and for others is 100 ms.

6. The different sensitivity of two modes to Al_2O_3 thickness

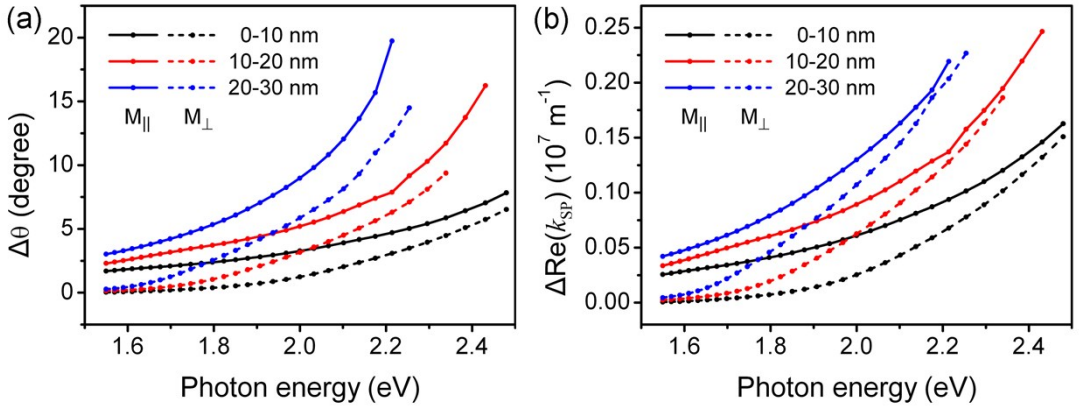

Figure S7. The increment of radiation angles (a) and wave vectors (b) of two modes caused by the increase of Al_2O_3 thickness (0-10 nm, 10-20 nm, and 20-30 nm) as a function of photon energy. The solid lines and dashed lines indicate the longitudinal mode and the transverse mode, respectively. The increment of both radiation angle and wave vector for longitudinal mode is larger than that for transverse mode by increasing the same Al_2O_3 thickness (comparing the solid and dashed lines of the same color), i.e., the radiation angle and the wave vector of longitudinal mode are more sensitive to the change of Al_2O_3 thickness.

7. The electric field distributions of longitudinal mode for different wavelengths and different Al_2O_3 thicknesses

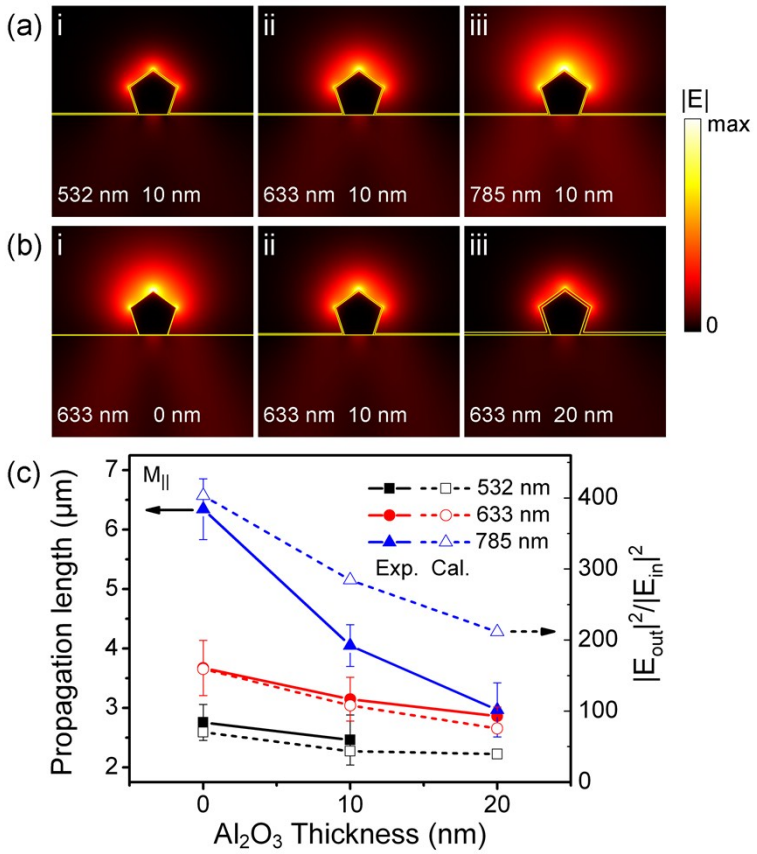

Figure S8. (a, b) The electric field distributions of longitudinal mode on glass-supported Ag NWs for Al_2O_3 thickness of 10 nm under different wavelengths (532, 633, and 785 nm), and for different Al_2O_3 thicknesses (0, 10, and 20 nm) under 633 nm wavelength. (c) Solid symbols: the experimental propagation lengths of the longitudinal mode for different excitation wavelengths and different Al_2O_3 thicknesses. Hollow symbols: the calculated ratio of the integration of $|E|^2$ outside and inside the Ag NW (only the electric field above the substrate is included, due to the nonconvergence of the wave in the substrate). The NW radius in simulation is 170 nm.